International Journal of Applied Pharmaceutics

ISSN- 0975-7058 Vol 14, Issue 4, 2022

Original Article

FORMULATION AND OPTIMIZATION OF CERITINIB LOADED NANOBUBBLES BY BOX-BEHNKEN DESIGN

PONNAGANTI MURALIKRISHNA[1], ANCHA KISHORE BABU[2], PALANATI MAMATHA[3]

[1]Shridhar University, Chirava Pilani Road, Pilani 333031, Rajasthan, India, [2]Raffles University, Japanese Zone, NH 8, Neemrana 301020, Rajasthan, India, [3]Teegala Ram Reddy College of Pharmacy, Pragathi Colony, Meerpet, Hyderabad 500097, Telangana, India
Email: akishorebabu@gmail.com

Received: 10 Feb 2022, Revised and Accepted: 26 Apr 2022

ABSTRACT

Objective: Ceritinib is an anaplastic lymphoma kinase (ALK) inhibitor used to treat lung cancer. In the current research, the ceritinib-loaded nanobubbles were prepared by using perfluorobutane for inner core and medium molecular weight chitosan for the shell**.**

Methods: A 3^3Box-Behnken design was used to determine the influence of L-α-Phosphatidylcholine (A), the concentration of chitosan (B) and concentration of palmitic acid (C) factors affecting particle size, and polydispersity index. The individual effects of these factors on particle size and polydispersity index were depicted in perturbation plot, response surfaces and counterplots based on Derringer's desirability approach.

Results: The extreme desirability function value was obtained at A: 1.31 % w/v, B: 3.00 % w/v, C: 1.5 % W/V. Three batches of formulation were prepared in accordance to the desirability function and evaluated. TEM images revealed the superficial morphology and core-shell structure of nanobubbles in the size range of 150-200 nm. Nanobubbles were able to load ceritinib with an encapsulation efficiency of 79.12 % and a loading capacity of 19.2 %. The nanobubbles released about 95.67 % drug in 24h. The *in vitro* cellular uptake study results show the enhanced cellular uptake of ceritinib with ultrasound from nanobubbles. *In vitro* cytotoxicity study results indicated that ultrasound-assisted nanobubbles can effectively release in the cells with high sensitivity.

Conclusion: Chitosan-based ceritinib nanobubbles, therefore, offer a remarkable tool for the development of ultrasound-responsive formulations that deliver drugs to the target.

Keywords: Ceritinib, Lung cancer, Chitosan nanobubbles, Box-Behnken design, *In vitro* cellular uptake study, *In vitro* cytotoxicity study

DOI: https://dx.doi.org/10.22159/ijap.2022v14i4.44388. Journal homepage: https://innovareacademics.in/journals/index.php/ijap

INTRODUCTION

Oral drug administration has got several benefits over other routes of administration. This route is non-invasive, safer, and comfortable, do not require a skilled person to administer, and dose adjustments can be tailor-made to suit the individual patient and hence it is most patient compliant [1]. The recent advance in nanotechnology has led to the development of a targeted drug delivery system. However, targeting a molecule to a particular site using a drug delivery system effectively requires a specialized drug delivery system [2]. Nanoparticle-based drug delivery systems form the crux of nanomedicine [3]. Nanobubbles are defined as bubbles with a diameter of less than one nanometer. These nanobubbles are 70-120 nanometers in size, and are 2500 times smaller than one grain of salt. The materials used to generate these nanobubbles can be any gas and any liquid. Nanobubbles, because of their size, contain unique characteristics for improving several physicals, chemical, and biological processes [4]. Despite their relatively small size, nanobubble formulations possess discrete properties that make them especially beneficial for improving productivity in pharmaceutical and agricultural settings. Nanobubbles owing to smaller size those possess enhanced stability, surface charge, neutral buoyancy, etc. Recently, ultrasound-guided delivery of drugs delivered through nanocarriers has received increasing attention as a method of improving therapeutic treatment. The ultrasonic field has been used in conjunction with microbubbles, microscopic spherical structures filled with gas and stabilized by a shell, to enhance the action of the ultrasonic field. In addition, nanobubbles may possess enhanced stability and a longer residence in systemic circulation [5].

The active ingredient in ceritinib, a drug developed by Novartis, for treating ALK-positive metastatic NSCLC patients. Clinically effective ceritinib needs a delivery system that can deliver both oral and peroral. A good oral dosage form should be able to produce a high bioavailability combined with low inter-and intra-subject variability in absorption. Furthermore, ideal systems for BCS class IV should deliver therapeutic concentrations of drugs at safe dose volumes for intravenous administration [6, 7]. A variety of types of nanobubbles have been described in previous studies. Many of these materials have only recently been identified.

Chemicals used in these nanobubbles pose a risk to human beings. To prepare the nanobubbles, it is important to take into account their biocompatibility and safety [8, 9].

Chitosan has gained attention because of its natural origin, biodegradability, biocompatibility, extremely low immunogenicity and antibacterial properties. Chitosan is a N-deacetylated derivative of chitin, which is one of the most abundant biological materials [10, 11]. Chitosan further has direct and indirect anti-cancer properties, making it a better drug carrier. With regards to the study, we aimed to develop ceritinib-loaded chitosan nanobubbles with suitable physicochemical properties and sizes in order to enhance the therapeutic utility of the drug.

MATERIALS AND METHODS

Preparation of ceritinib loaded nanobubbles

Ceritinib (100 mg) was dissolved in perfluorobutane core using ethyl alcohol as a co-solvent to facilitate drug dissolution. L-α-Phosphatidylcholine and palmitic acid were dissolved in ethanol and added to the ceritinib-perfluorobutane solution to form a pre-emulsion. This emulsion was suitably diluted with ultrapure water and homogenized using a high shear homogenizer (T 25 digital ULTRA-TURRAX®) for 5 min at 12000 rpm in an ice bath. Finally, a chitosan solution at pH 5.0 was added dropwise. The formed nanobubbles formulation was purified by ultrafiltration using a TCF2 instrument (Millipore) with a membrane cut-off diameter of 100000. Finally, a PluronicF68 solution (0.01% v/v) was added to the nanobubbles formulation as a stabilizing layer. Afterward, the system was subjected to incubation for 30 min.

Optimization of critical parameters using design of experiments

In this study, response surface methodology utilizing Box-Behnken design (BBD) was employed to investigate the influence of three

controlled variables (A), chitosan concentration (B), and palmitic acid concentration (C) on two outcome variables, particle size (PLS) and polydispersity index (PI) of ceritinib loaded nanobubbles [12, 13] [table 1]. As described by the BBD model, 17 experiments were randomly arranged by Design Expert® software. The experimental conditions for all the trials are presented in table 2.

Table 1: Box-Behnken design

Factors			Levels		
		Units	Low	Intermediate	High
A	Conc. of L-α-Phosphatidylcholine	w/v	1	1.5	2
B	Conc. of Chitosan	w/v	1	2	3
C	Conc. of palmitic acid	w/v	0.5	1	1.5
Responses			Goal		
Y1	PLS	nm	Decrease		
Y2	PI	-	Decrease		

Table 2: Observed responses of trial experiments as per Box-Behnken design

Run	A (w/v)	B (w/v)	C (w/v)	PLS (nm)	PI
1	1.5	2	1	346.48	0.22
2	1.5	3	1.5	224.78	0.2
3	1	1	1	292.72	0.29
4	1	2	0.5	376.12	0.44
5	1.5	2	1	349.76	0.24
6	1	3	1	256.72	0.28
7	2	3	1	273.78	0.32
8	1	2	1.5	330.54	0.18
9	2	2	1.5	351.12	0.27
10	2	1	1	308.12	0.34
11	1.5	2	1	349.12	0.21
12	1.5	3	0.5	266.72	0.39
13	1.5	1	1.5	266.42	0.19
14	1.5	2	1	347.38	0.21
15	2	2	0.5	396.56	0.42
16	1.5	1	0.5	303.59	0.41
17	1.5	2	1	350.76	0.23

Data analysis

The obtained results were subject to statistical analysis [14]. All the parameters were expressed as mean±standard deviation (SD). The parameters were further subjected to statistical analysis using Graph Pad Prism software (Graph Pad Software Inc., San Diego, CA). The p-value is calculated using the sampling distribution of the test statistic under the null hypothesis, the sample data, and the two-sided test. If the p-value is 0.05, that means 5% of the time, would see a test statistic at least as extreme as the one found if the null hypothesis was true.

Each response parameter can be evaluated by the quadratic model using multiple regression analysis, as shown in equation 1.

$$Y = A_0 + A_1 X_1 + A_2 X_2 + A_3 X_3 + A_4 X_1^2 + A_5 X_2^2 + A_6 X_3^2 + A_7 X_1 X_2 + A_8 X_1 X_3 + A_9 X_2 X_3 (1)$$

Were Y–Response parameter

A_0–Intercept

A_1–A_9–regression coefficients

X_1, X_2 and X_3–Main influencing factors

X_1X_2–Interactive effect

X_1^2, X_2^2, X_3^2–Quadratic effect

Optimization

The optimal points for the independent variables were attained using the numerical optimization technique by setting restrictions on the response parameters and influencing factors.

Characterization of nanobubbles formulation

Determination of PLS, PI and zeta potential (ZEP) [15], Transmission electron microscopy (TEM) [16], Encapsulation efficiency (ETE) and loading capacity (DLC), [17], Viscosity and refractive index of nanobubbles, [18] and DSC [19] was determined by the following procedure from reference.

***In vitro* release (IVR) of the drug in the absence and presence of ultrasound**

By the dialysis bag technique at 37 °C, the IVR data of ceritinib from the nanobubbles was measured both in the presence and absence of ultrasound. All the samples were spectrophotometrically evaluated to determine the drug amount [20].

Ultrasound stability of ceritinib nanobubbles

Ceritinib-loaded nanobubbles were induced through ultrasound stimulation with an oscillation frequency of 2.5±0.2 MHz, an acoustic pressure distribution of 2.5 * 0.2 MPa, a nominal frequency of 50 Hz, and a nominal power of 30W. Using optical microscopy, the formulations were examined before and after ultrasound exposure, for 30 seconds, 1, 2, 3, 4 and 5 min at 37 °C, following a 10-minute rest period, using morphological analysis as part of evaluating the integrity of the nanobubbles [21].

Evaluation of the stability of ceritinib nanobubbles

The stability of ceritinib nanobubbles was evaluated at different temperatures (4 °C, 25 °C and 40 °C) for 1 mo. The content of ceritinib, encapsulation efficiency and the average particle size of ceritinib-loaded nanobubbles were determined on the 1st, the 10th and the 30th day. The appearance of ceritinib-loaded nanobubbles was also observed using optical microscopy to evaluate the integrity of their structures [22].

Determination of haemolytic activity

Human blood was used to assess the hemolytic activity of chitosan nanobubbles. As different concentrations of nanobubbles formulations (1, 2, 4, 6, 8 and 10%), were added to a suspension of erythrocytes (30%, v/v) in phosphate buffer at pH 7.4. To obtain the

haemolytic control, a suspension of erythrocytes (30%, v/v) in phosphate buffer pH 7.4 was used as the blank condition, to which an excess of ammonium chloride was added to complete haemolysis. During the incubation process, the samples were incubated at 37 degrees Celsius for two hours. Following centrifugation for 10 min at 3000 RPM, the supernatants were analyzed using a spectrophotometer with a wavelength of 543 nm [23]. Percent hemolysis is calculated using the equation.

$$\% \, Hemolysis = \frac{ABS_{Sample} - ABS_0}{ABS_{100} - ABS_0} \, X \, 100$$

Where ABS_0 and ABS_{100} are the absorbances of the solution at 0 and 100 % hemolysis, respectively.

In vitro cellular uptake study

The cellular uptake of ceritinib and ceritinib-loaded nanobubbles was assessed through confocal laser scanning microscopy. At various time intervals, cells were photographed by using confocal laser scanning microscopy under filtered blue light with excitation wavelengths of 405 nm [24]. Using fluorescent microplates, the fluorescent intensity was measured at excitation wavelengths of 503 nm and emission wavelengths of 528 nm. There was a triplicate of every trial.

In vitro cell cytotoxicity assay

After incubation in DMEM containing 10% fetal calf serum, the cells were transferred into 96-well plates at 5 104 cells per well under 5% CO2 atmosphere at 37 °C. Blank, Ceritinib dissolved in DMSO, Ceritinib nanobubbles without sonication (50 *M), and Ceritinib nanobubbles with sonication (50 *M) at different concentrations were all added into the wells with a 9:1 ratio of culture medium to nonmedia after incubation to fill the wells. We treated each well with 5 mg/ml MTT for 4 h after incubation for 24 and 48 h, respectively. The medium was discarded and the solution was dissolved in 25 °C dimethyl sulfoxide. We measured absorbance at 570 nm with a Microplate Absorbance Reader (Model 680, Bio-Rad Laboratories, Hercules, CA).

RESULTS AND DISCUSSION

It is evident from the preliminary experiments that the conc. of L-α-Phosphatidylcholine (A), conc. of chitosan (B) and conc. of palmitic acid (C), had a significant effect on the PLS and PI of nanobubbles. It was difficult to replicate those procedures because of the difficulty in controlling the variables for the preparation of nanobubbles. The PLS and PI were regarded as the main indicators for the evaluation of ceritinib-loaded nanobubbles. Hence it is essential to optimize the formulation variables to obtain desired results.

RSM optimization

Statistical analysis

A sequence of seventeen trials was executed as per a 3^3BBD [table 2]. The PLS (Y1) for all the trials was found to be in the range of 224.78-396.56 nm. Similarly, the range of PI (Y2) was 0.18-0.44 [table 3].

Table 3: Regression equations for the responses–particle size and polydispersity index

Dependent variable	Regression equation
Y1	348.1584+9.185 A–18.6063 B–21.2663 C+16.10355 A^2–82.1039 B^2
Y2	0.222+0.02 A-0.005 B-0.1025 C+0.0275 AC+0.05775 A^2+0.02775 B^2+0.04775 C^2

Particle size

The size of nanocarriers is a main factor which influences their permeation and retention through various tumor tissues and organs [25]. The PLS of the nanobubbles was found to be in the range of 224.78–396.56 nm. The individual effects of A, B and C on PLS were depicted in PP. Fig. 1-3 clearly indicated that C has the main and major effect on PLS followed by C has an intermediate effect and A has little effect.

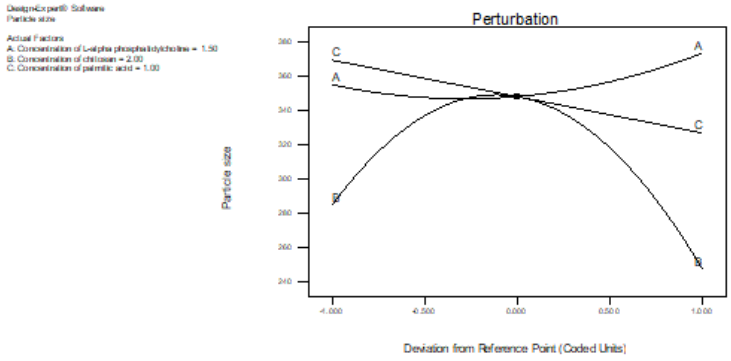

Fig. 1: Two-dimensional perturbation plot–effect of A, B and C on particle size

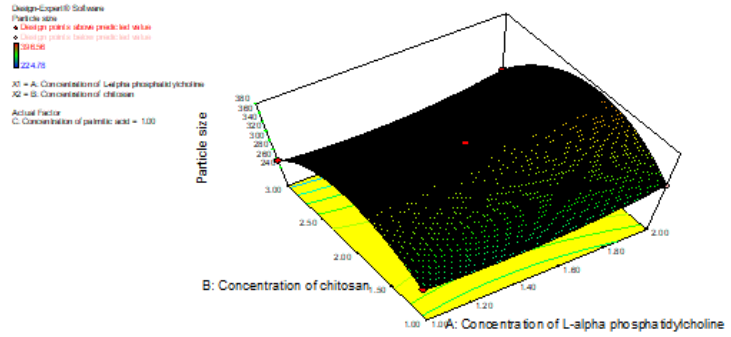

Fig. 2:3D-RSP showcasing the effect of A and B on particle size at a constant level of C

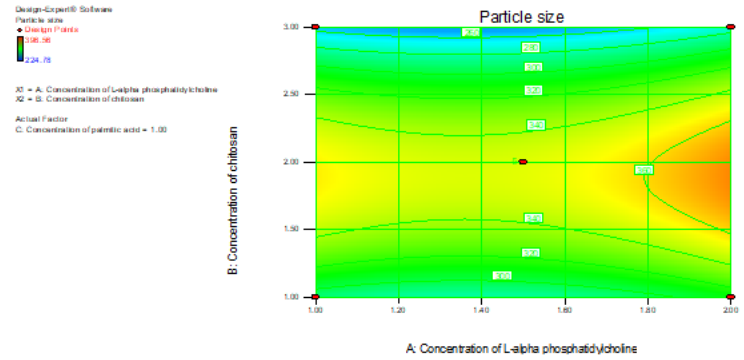

Fig. 3: CP showcasing the impact of A and B on particle size at a constant level of C

Polydispersity index (Y2)

The PI values of nanobubbles were found to be in the range of 0.18–0.44 as presented in table 4. Fig. 4 clearly indicated that C has the main and major effect on PI followed by A and Bhave little effect. The interactive effect of A and C (AC) at a constant level of B on particle size is as shown in fig. 5 and 6.

Optimization

The extreme Derringer's desirability function value was obtained at A: 1.31 % w/v, B: 3.00 % w/v, C: 1.5 % w/v with the conforming D value of 0.999. To confirm the appropriateness of the model, three executive bathes of nanobubbles were prepared under optimal conditions [26] [table 4].

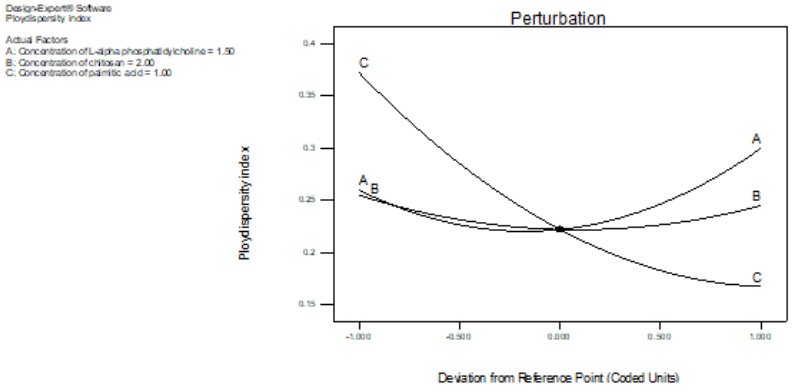

Fig. 4: 2D PP–Effect of A, B and C on polydispersity index

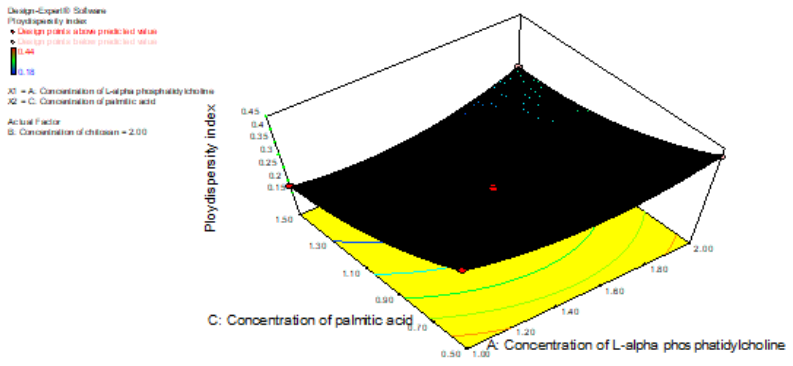

Fig. 5: 3D-RSP showcasing the influence of A and C on polydispersity index at a constant level of B

Table 4: Optimum conditions attained by applying restrictions on response parameters

Independent variables	Optimized values	Predicted values		Actual values			
		PLS (Y1) nm	PI (Y2)	Batch	PLS (Y1) nm±SD	PI (Y2)±SD	ZP (mV)±SD
Concentration of L-α-Phosphatidylcholine	1.31	224.994	0.180	B1	232.46±5.82	0.20±0.005	27.4±2.23
Concentration of Chitosan	3.00			B2	229.56±4.12	0.21±0.005	25.7±1.18
Concentration of palmitic acid	1.5			B3	233.48±3.46	0.19±0.005	27.9±2.26

Results are represented by mean±SD (n = 3). (p<00.5)

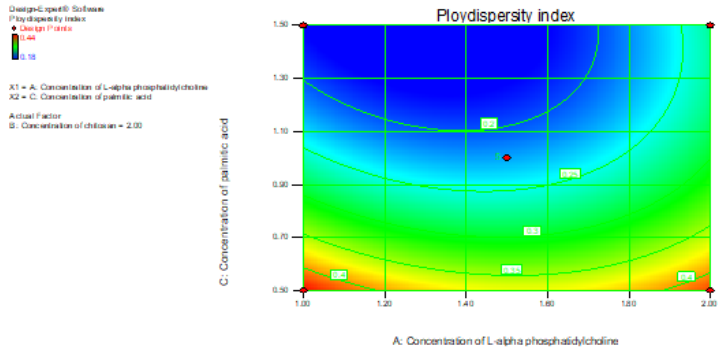

Fig. 6: CP showcasing the impact of A and C on polydispersity index at a constant level of B

The particle size of all the batches of ceritinib nanobubbles was found to be similar with low polydispersity indices (table 5). The higher zeta potential values indicate the high storage stability of nanobubbles. The positive values of the zeta potential confirm the presence of chitosan on the surface [27].

TEM images revealed the superficial morphology and core-shell structure of nanobubbles in the size between 150-200 nm. Moreover, the particle size determined by the dynamic light scattering method is correlated well with the TEM measurement (fig. 7).

Nanobubbles were able to load ceritinib with an encapsulation efficiency of 79.12 % and a loading capacity of 19.2 %. The loading of ceritinib in the nanobubble structure did not significantly affect the viscosity of the formulations.

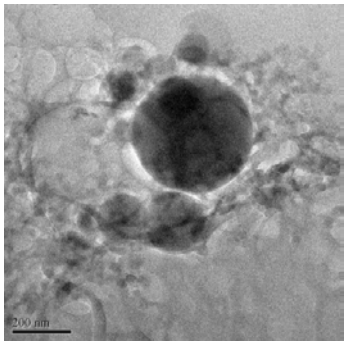

Fig. 7: TEM image of ceritinib nanobubbles

Table 5: Physical characteristics of nanobubbles

	Blank nanobubbles±SD	Ceritinib loaded nanobubbles±SD
Average particle size	218.34±4.88	232.46±5.82
Polydispersity index	0.19±0.005	0.20±0.005
Zeta potential	62.36±2.42	27.4±2.23
Encapsulation efficiency	-	79.12±4.36
Loading capacity	-	19.23±1.32

Results are represented by mean±SD (n = 3).

The DSC curve of ceritinib has shown a peak at 179.17 °C, corresponding to its melting point. The DSC curve of chitosan has shown an endothermic peak at 87.82 °C. The DSC curve of blank nanobubbles has shown two endothermic peaks. Chitosan nanobubbles displayed an endothermic peak at 98.34 °C, while chitosan peak appeared at 87.82 °C. The disappearance of the characteristic endothermic peak of the drug indicating the complete inclusion of the drug within the core structure (fig. 8).

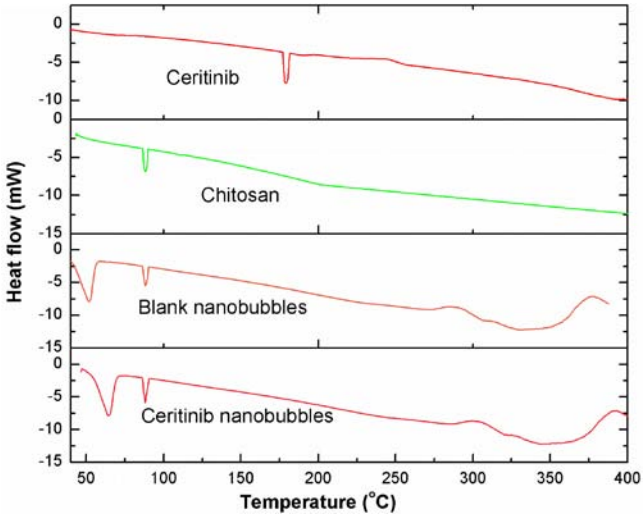

Fig. 8: DSC thermogram of ceritinib, Chitosan, blank nanobubbles and ceritinib loaded nanobubbles

The amount of drug released from nanobubbles was significantly higher than that from the ceritinib suspension. Significant difference was observed between the drug released from ultrasound assistance and non-ultrasound assistance. After 6 h, 54.54 % of ceritinib was released under sonication, whereas only 26.34 % were released without sonication. Without ultrasound, only 60.12 % of ceritinib was released after 24 h. In contrast, almost 95.67 % of ceritinib was released with ultrasound. The results suggested that ultrasound assistance may promote the release of ceritinib from the nanobubbles due to the cavitation effect (fig. 9).

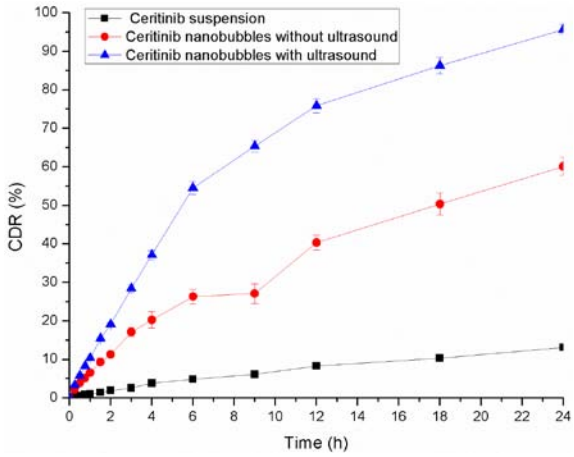

Fig. 9: *In vitro* drug release pattern with and without ultrasound assistance; results are represented by mean±SD (n = 3)

The stability of ceritinib-loaded nanobubbles was evaluated after exposure to ultrasound at different temperatures. After 5 min of sonication (2.5 MHz) at 25 °C, the morphology and structure Nanobubbles remains unaffected. On the contrary, at 37 °C, nanobubbles begin to disappear at 3 min and completely disappeared after 5 min of sonication, indicating a decrease in instability. This can be attributed to the low boiling point of perfluoropentane, this component might exist as a gas at 37 °C; however, the transition might be shifted to higher temperature values due to the small sizes of the nanobubbles. Furthermore, in the presence of ultrasound, the gas core undergoes a conversion from nanodroplet to bubble via a mechanism known as acoustic droplet formation.

The storage stability of ceritinib nanobubbles was evaluated at different temperatures (4 °C, 25 °C and 40 °C) for 1 mo. No significant change in drug content was observed at lower temperatures (table 6). All through the study, the PDI drug-loaded nanobubbles were <0.3, indicative of homogenous size distribution.

Table 6: Encapsulation efficiency, particle size, and polydispersity index of ceritinib nanobubbles stored at different temperatures

Temperature (°C)	Time (days)	Encapsulation efficiency (%)±SD	PLS (nm)±SD	PI±SD
4±1 °C	0	79.12±4.36	232.46±5.82	0.20±0.005
	15	78.34±1.87	236.78±2.23	0.21±0.005
	30	78.12±2.12	235.64±1.38	0.19±0.005
25±2 °C	0	79.12±4.36	232.46±5.82	0.20±0.005
	15	77.38±2.12	229.56±3.32	0.22±0.005
	30	77.12±3.12	236.78±2.12	0.21±0.005
40±2 °C	0	79.12±4.36	232.46±5.82	0.20±0.005
	15	72.34±1.68	253.56±8.89	0.24±0.005
	30	68.74±4.22	289.56±11.24	0.41±0.005

Results are represented by mean±SD (n = 3).

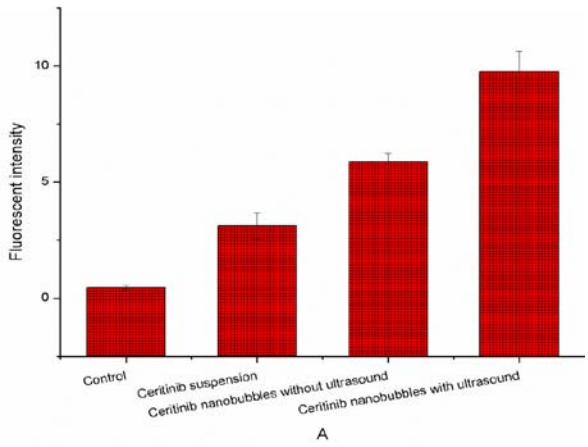

Fig. 10: Results of cellular uptake study, Results are represented by mean±SD (n = 3)

The aqueous suspensions of chitosan nanobubbles were found to be non-hemolytic up to the tested concentration of 5 mg/ml. Drug-loaded nanobubbles also showed a good safety profile with erythrocytes.

***In vitro* cellular uptake study**

The cellular uptake of ceritinib from nanobubbles formulation in HepG2 cells was determined using fluorescent intensity analysis. The fluorescent intensity data generated from HepG2 cells after incubation for 2 h is presented in fig. 24. Cells treated with Ceritinib Nanobubbles with ultrasound showed mean fluorescence intensity of 9.76 in HepG2 cells, which is 1.7 times higher than that treated with Ceritinib Nanobubbles without ultrasound. This data indicates the enhanced cellular uptake of ceritinib with ultrasound from nanobubbles (fig. 10).

***In vitro* cytotoxicity study**

HepG2 cells exhibited more than 98 % viability when exposed to capsaicin formulations at lower concentrations (10 µM), irrespective of the formulation. The cell viability was greater than 85 %, even at a concentration of ceritinib at 20 µM that might arise due to a low concentration than the minimum effective concentration. The IC50 values of free ceritinib, IB nanobubbles without ultrasound and IB nanobubbles with ultrasound were 92.32, 55.78 and 38.16µM. This result indicated that ultrasound-assisted nanobubbles can effectively release in the cells with high sensitivity [24] (fig. 11).

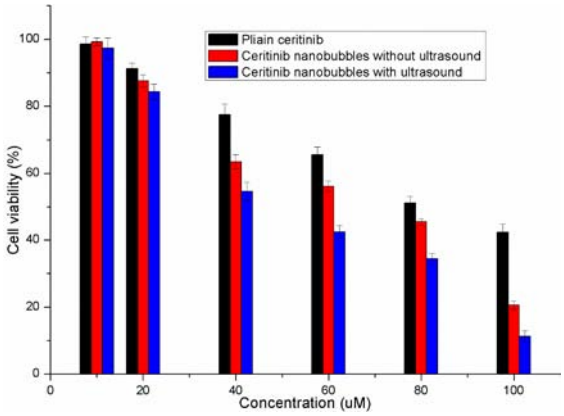

Fig. 11: *In vitro* cytotoxicity of plain ceritinib, ceritinib nanobubbles without ultrasound and with ultrasound, Results are represented by mean±SD (n = 3)

CONCLUSION

In this study, chitosan-shelled and perfluropentane-filled nanobubbles were developed for the delivery of the anticancer drug ceritinib. The formulation components were optimized with respect to PLS and PI using response surface methodology. Nanobubbles prepared under optimal conditions exhibited uniform particle size distribution. Compared with the solubility of ceritinib suspension, that of the ceritinib nanobubbles is significantly increased at different pH values. *In vitro* dissolution test demonstrated that compared with the suspension, ceritinib nanobubbles displays better dissolution profiles and higher gastrointestinal stability, leading to a significant increase in oral bioavailability. Moreover, *in vitro* cytotoxicity studies illustrated that ceritinib nanobubbles displayed superior growth inhibition of tumor cells.

FUNDING

Nil

AUTHORS CONTRIBUTIONS

All the authors have contributed equally.

CONFLICT OF INTERESTS

Declared none

REFERENCES

1. Joshi V, Sulthana F, Ramadas D. Oral delivery of silver nanoparticles– a review. Asian J Pharm Clin Res. 2021;14(11):9-14. doi: 10.22159/ajpcr.2021.v14i11.42986.
2. Bhowmik H, Nagasamy Venkatesh D, Kuila A, Kammari Harish Kumar N. A review. Int J Appl Pharm. 2018;10(4):207-1.
3. Hussain M, Sarma A, Rahman SS, Siddique AM, Eeswari TP. Formulation and evaluation of ethambutol polymeric nanoparticles. Int J App Pharm. 2020;12(4):207-17. doi: 10.22159/ijap.2020v12i4.36845.
4. Cavalli R, Soster M, Argenziano M. Nanobubbles: a promising efficient tool for therapeutic delivery. Ther Deliv. 2016 Feb;7(2):117-38. doi: 10.4155/tde.15.92, PMID 26769397.
5. Cavalli R, Bisazza A, Lembo D. Micro- and nanobubbles: a versatile non-viral platform for gene delivery. Int J Pharm. 2013;456(2):437-45. doi: 10.1016/j.ijpharm.2013.08.041, PMID 24008081.
6. Fontana D, Ceccon M, Gambacorti Passerini C, Mologni L. Activity of second-generation ALK inhibitors against crizotinib-resistant mutants in an NPM-ALK model compared to EML4-ALK. Cancer Med. 2015 Jul;4(7):953-65. doi: 10.1002/cam4.413, PMID 25727400.
7. Friboulet L, Li N, Katayama R, Lee CC, Gainor JF, Crystal AS, Michellys PY, Awad MM, Yanagitani N, Kim S, Pferdekamper AC, Li J, Kasibhatla S, Sun F, Sun X, Hua S, McNamara P, Mahmood S, Lockerman EL, Fujita N, Nishio M, Harris JL, Shaw AT, Engelman JA. The ALK inhibitor ceritinib overcomes crizotinib resistance in non–small cell lung cancer. Cancer Discov. 2014 Jun 1;4(6):662-73. doi: 10.1158/2159-8290.CD-13-0846, PMID 24675041.
8. Li D, Wu X, Yu X, Huang Q, Tao L. Synergistic effect of non-ionic surfactants tween 80 and PEG6000 on cytotoxicity of insecticides. Environ Toxicol Pharmacol. 2015;39(2):677-82. doi: 10.1016/j.etap.2014.12.015, PMID 25699500.
9. Ramot Y, Haim Zada M, Domb AJ, Nyska A. Biocompatibility and safety of PLA and its copolymers. Adv Drug Deliv Rev. 2016;107:153-62. doi: 10.1016/j.addr.2016.03.012, PMID 27058154.
10. Ravi Kumar MNVR. A review of chitin and chitosan applications. React Funct Polym. 2000;46(1):1-27. doi: 10.1016/S1381-5148(00)00038-9.
11. Van LA, Knoop RJ, Kappen FH, Boeriu CG. Chitosan films and blends for packaging material. Carbohydr Polym. 2015;116:237-42.
12. Roy RK. A primer on the Taguchi method. Society of Manufacturing Engineers; 2010.
13. Dhiman S, Verma S. Optimization of melt-in-mouth tablets of levocetirizine dihydrochloride using response surface methodology. Int J Pharm Pharm Sci. 2012;4.
14. Nazzal S, Khan MA. Response surface methodology for the optimization of ubiquinone self-nano emulsified drug delivery system. AAPS PharmSciTech. 2002 Mar;3(1):E3. doi: 10.1208/pt030103, PMID 12916956.

15. Zhang X, Wang Q, Wu Z, Tao D. An experimental study on size distribution and zeta potential of bulk cavitation nanobubbles. Int J Miner Metall Mater. 2020;27(2):152-61. doi: 10.1007/s12613-019-1936-0.
16. Uchida T, Oshita S, Ohmori M, Tsuno T, Soejima K, Shinozaki S, Take Y, Mitsuda K. Transmission electron microscopic observations of nanobubbles and their capture of impurities in wastewater. Nanoscale Res Lett. 2011;6(1):295. doi: 10.1186/1556-276X-6-295, PMID 21711798.
17. Marano F, Argenziano FR, AAdamini, Bosco, Rinella L, Fortunati N, Cavalli R, Catalano MG. Doxorubicin-loaded nanobubbles combined with extracorporeal shock waves: basis for a new drug delivery tool in anaplastic thyroid cancer. Thyroid. 2016;26:705–16.
18. Chandralingam R. An investigation of nanobubbles in aqueous solutions for various applications. Appl Nanosci. 2018;8(2):1557-67. doi: 10.1007/s13204-018-0831-8.
19. Lentacker I, De Smedt SC, Sanders NN. Drug-loaded microbubble design for ultrasound-triggered delivery. Soft Matter. 2009;5(11):2161-70. doi: 10.1039/b823051j.
20. Batchelor DVB, Abou-Saleh RH, Coletta PL, McLaughlan JR, Peyman SA, Evans SD. Nested nanobubbles for ultrasound-triggered drug release. ACS Appl Mater Interfaces. 2020;12(26):29085-93. doi: 10.1021/acsami. 0c07022, PMID 32501014.
21. Park B, Yoon S, Choi Y, Jang J, Park S, Choi J. Stability of engineered micro or nanobubbles for biomedical applications. Pharmaceutics. 2020;12(11):1089. doi: 10.3390/pharmaceutics12111089, PMID 33202709.
22. Oh SH, Kim JM. Generation and stability of bulk nanobubbles. Langmuir. 2017;33(15):3818-23. doi: 10.1021/acs. langmuir.7b00510, PMID 28368115.
23. Halina, Kizek, Rene A. Rapid method for the detection of sarcosine using SPIONs/Au/CS/SOX/NPs for prostate cancer sensing. Uhlirova, Dagmar and Stankova, Martina and Docekalova, Michaela and Hosnedlová, Božena and Kepinska, Marta and Ruttkay-Nedecky, Branislav and Ruzicka, Josef and Fernández, Carlos and Milnerowicz. Int J Mol Sci. 2018;19:3722.
24. Tomar J, Rastogi V, Garg PC. *In vitro* cytotoxicity assay of crude extract of ethnobotanical mixtures used in the indigenous treatment of tuberculosis. Int J Pharm Clin Res. 2021;14(1):9-14.
25. Kishore Babu A, Bhanu Teja B, Ramakrishna B, Balagangadhar B, Vijay Kumar V, Venkat Reddy V. Formulation and evaluation of double-walled microspheres loaded with pantoprazole, IJRPC. 2011;1(4):770-9.
26. Mamatha P, Arun Kumar J, Bhikshapathi DVRN. Design and optimization of Ibrutinib solid lipid nanoparticles using design of experiment, IJBPAS. 2021;10(9):723-37.
27. Hoven VP, Tangpasuthadol V, Angkitpaiboon Y, Vallapa N, Kiatkamjornwong S. Surface-charged chitosan: preparation and protein adsorption. Carbohydr Polym. 2007 Mar 1;68(1):44-53. doi: 10.1016/j.carbpol.2006.07.008.